Computer Physics Communications 300 (2024) 109181

Contents lists available at ScienceDirect

Computer Physics Communications

journal homepage: www.elsevier.com/locate/cpc

Computational Physics

Arbitrary controlled re-orientation of a spinning body by evolving its tensor of inertia ☆

Igor A. Ostanin [a,*], Matthias Sperl [b]

[a] Multi-Scale Mechanics (MSM), Faculty of Engineering Technology, MESA+, University of Twente, P.O. Box 217, Enschede, 7500 AE, the Netherlands
[b] Institute of Materials Physics in Space, German Aerospace Center DLR, Cologne,51170, Germany

A R T I C L E I N F O

Dataset link: https://bitbucket.org/mercurydpm/mercurydpm/src/master

Keywords:
Optimal control
Rigid body mechanics

A B S T R A C T

Bodies with the nonspherical tensor of inertia (TOI) exhibit a variety of rotational motion patterns, including chaotic motion, stable periodic (quasi-periodic) rotation, unstable rotation around the direction close to the body's second principal axis, featuring a well-known tennis-racket (also known as Garriott-Dzhanibekov [1]) effect – series of seemingly spontaneous 180 degrees flips. These patterns are even more complex if the body's TOI is changing with time. Changing a body's TOI has been discussed recently as a tool to perform controllable Garriott-Dzhanibekov flips and similar maneuvers. In this work, the optimal control of the TOI of the body (spacecraft, or any other device that admits free rotation in three dimensions) is used as a means to perform desirable re-orientations of a body with respect to its angular velocity. Using the spherical TOI as the initial and final point of the maneuver, we optimize the parameters of the maneuver to achieve and stabilize the desired orientation of the body's principal axes with respect to spin angular velocity. It appears that such a procedure allows for finding arbitrarily complex maneuver trajectories of a spinning body. In particular, intermediate axis instability can be used to break the alignment of the body's principal axis and the axis of rotation. Such maneuvers do not require utilization of propellants and could be straightforwardly used for attitude control of a spin-stabilized spacecraft. The capabilities of such a method of angular maneuvering are demonstrated in numerical simulations.

1. Introduction

From antiquity, humankind possesses empirical knowledge of how to manipulate the dynamic rotational motion of a body or a mechanism by adjusting its mass distribution. Some impressive examples can be found in acrobatic sports – martial arts, figure skating, synchronized diving, etc. However, this large array of practical knowledge was collected in presence of gravity, complicating observation of three-dimensional rotations of solid bodies due to insufficient available observation time. In more modern times, gyroscope frames and drop towers facilitated some systematic research on the topic. The beginning of the era of orbital spaceflights sparked a new wave of interest in these phenomena, however, direct "trial and error" research in space still remains too expensive for the implementation of exhaustive experimental programs on the topic.

It is worth noting that the fundamental equations of rigid body dynamics, suggesting different types of rotational motion control, were discussed rather early [2] - more than a century before the era of spaceflight, predictive numerical modeling of rigid body mechanics, and almost two decades before the emergence of the first gyroscope.

Subsequently, attitude control of a spinning body became an important challenge for aerospace technology. Up-to-date satellites, spacecraft, and other systems capable of performing major orientation maneuvering do so by introducing external torques, using small reactive thrust engines [3]. Such an angular positioning system can be used only a limited number of times, namely – until the propellant is fully consumed. Alternatively, the existing inertial systems (reaction wheels and similar devices) are capable to adjust or stabilize the attitude very precisely, given small drift angular velocities, but cannot be used to terminate the fast rotation of a spacecraft. These, as well as some less

☆ The review of this paper was arranged by Prof. Andrew Hazel.

* Corresponding author.
E-mail addresses: i.ostanin@utwente.nl (I.A. Ostanin), matthias.sperl@dlr.de (M. Sperl).

https://doi.org/10.1016/j.cpc.2024.109181
Received 28 November 2023; Received in revised form 12 March 2024; Accepted 15 March 2024
Available online 21 March 2024

common systems (e.g. passive ones using the gradient of drag forces of the thin atmosphere, gravitational force gradient, yoyo de-spins, etc.), fall into two categories (see, e.g. [3], [4]):

- The ones using "external" moments $\mathbf{M}_i^{ext}$ of different nature. The conservation of angular momentum $\mathbf{L} = \mathbf{I}\dot{\boldsymbol{\omega}}$ in this case can be written as[1]:

$$\mathbf{I}\dot{\boldsymbol{\omega}} = \sum_i \mathbf{M}_i^{ext} \quad (1)$$

- the ones redistributing the conserving angular momentum between the main body and its special rotating mechanical parts:

$$\mathbf{I}\dot{\boldsymbol{\omega}} = -\sum_i \mathbf{I}_i \dot{\boldsymbol{\omega}}_i \quad (2)$$

Until recently, the third possibility has been largely neglected - altering magnitude and direction of the spin angular velocity by changing the TOI:

$$\mathbf{I}\dot{\boldsymbol{\omega}} = -\dot{\mathbf{I}}\boldsymbol{\omega} \quad (3)$$

The fundamental difference with (2) is that the change of the TOI is achieved by symmetric redistribution of weights using forces that do not create internal moments, while the reaction wheels and other similar systems imply net **rotation** of the masses by nonzero internal moments.

The changes in the TOI can dramatically change the behavior of a spinning body. The presence of the deviatoric part of the TOI causes misalignment of the angular velocity and angular momentum of a spinning body, leading to chaotic motion [5], except the special cases of stable periodic rotations around major or minor principal axes (or quasi-periodic rotation/wobbling about the axes close to these principal axes). The rotation about the direction close to the intermediate principal axis causes the instability [6], leading to a well-known tennis-racket effect – a series of quasi-periodic 180 degrees flips of the body orientation with respect to its spin angular velocity. Therefore, a controlled mass redistribution leading to the transformation of the major or minor principal axis into the intermediate one can be an efficient tool of orientation control.

This idea has been highlighted for the first time in [7,8], although the idea to use moving mass mechanisms for stabilization/de-tumbling emerged even earlier [9,10]. The method developed further, in particular, in the work [11] that suggested to use Garriott-Dzhanibekov flips for controllable re-orientation of a space sail.

This concept was revisited in 2017 by P. Trivailo et al. [12] who have demonstrated its feasibility in a numerical simulation. The same collective of authors have later developed and generalized it in [1]. They indicated a few different particular maneuvers that could be accomplished by altering a body's TOI. However, all the existing works dealt so far only with the particular cases of orientation control, i.e. switching between the pre-defined axes of possible stable rotation.

In this work, we demonstrate the straightforward way to achieve **arbitrary** angular re-orientations of a spinning body with respect to its rotation axis, by changing a body's TOI. The key idea is to have a **spherical** TOI at the initial and the final moment of the maneuver. This way both the initial and final states are characterized by stable periodic rotation. The desirable angular re-orientation is then achieved by optimization of the parameters of TOI's time evolution between the initial and the final state.

In the context of spacecraft attitude control and maneuvering, such a method has several attractive features. In contrast with the existing systems, the system manipulating the spacecraft's TOI is capable in principle of guiding the body toward an arbitrarily selected orientation with respect to its axis of rotation by redistributing the energy between the chemical storage and the kinetic energy of the body's rotation. Such angular maneuvers are achieved without spending the mass of the propellant and with zero net energy losses, other than relatively small heat losses in electrical circuits and frictional mechanical contacts. Among other important features of such a method of maneuvering is the possibility to change the TOI by displacing the payload rather than dead weights, and the insensitivity of the maneuver structure to the absolute value of the spacecraft's angular momentum - see the in-depth discussion below.

To demonstrate the capabilities of this approach, we have developed a special simulation-guided optimization framework, based on the implementation of nonspherical particle dynamics within the open-source code MercuryDPM [13]. All the simulation codes presented here are freely available via MercuryDPM repository at https://www.mercurydpm.org/.

The framework convincingly demonstrates the impressive capabilities of attitude correction by optimal control of the body's TOI. Necessary manipulations with the TOI do have a straightforward mechanical interpretation and can be implemented in a real spacecraft.

The paper is organized as follows. Section 2 provides the necessary theoretical background and discusses the methodology used; the details related to the numerical methods used are presented in the supplementary material. Section 3 discusses the results of numerical simulations, demonstrating the validity of our approach. Section 4 gives the larger picture of the fundamental value and possible applications of our findings.

2. Methods

In this section we will consider the major components of the suggested methodology of optimal control of angular orientation of a spinning body. Finer technical details are discussed in the Supplementary information.

Maneuvering by changing the TOI – general considerations Unlike the total mass of an isolated mass distribution (body or mechanism), its TOI can in principle be changed by altering its geometry. Hereafter we will still use the term "rigid" for the motion of the body that changes its TOI, although the use of such a terminology becomes ambiguous.

By "change" of the TOI here and below we will understand the change in its principal components. It is important to note, however, that simple geometric considerations show that principal components of inertia can not be changed independently. For example, scaling the mass distribution along the principal direction 1 affects both I_2 and I_3. It, therefore, makes sense to choose the control parameters as mass distribution scaling factors $q_i(t)$:

$$\begin{aligned} I_1 &= \frac{I_0}{2}(q_2(t)^2 + q_3(t)^2), \\ I_2 &= \frac{I_0}{2}(q_1(t)^2 + q_3(t)^2), \\ I_3 &= \frac{I_0}{2}(q_1(t)^2 + q_2(t)^2). \end{aligned} \quad (4)$$

It is also easy to see that without loss of generality we can accept $q_3(t) = 1$, as it would only contribute to a scaling multiplier of the angular velocity (see, e.g. [14]). The scaling of the principal components of the TOI and their time derivatives is then given as:

$$\begin{aligned} I_1 &= \frac{I_0}{2}(1 + q_2(t)^2), \dot{I}_1 = I_0 q_2(t)\dot{q}_2(t) \\ I_2 &= \frac{I_0}{2}(1 + q_1(t)^2), \dot{I}_2 = I_0 q_1(t)\dot{q}_1(t) \\ I_3 &= \frac{I_0}{2}(q_1(t)^2 + q_2(t)^2), \dot{I}_3 = I_0(q_1(t)\dot{q}_1(t) + q_2(t)\dot{q}_2(t)) \end{aligned} \quad (5)$$

[1] The equations (1)-(3) are sketched here for a simple illustrative case of stable rotation. An analogue of (3) for an arbitrary 3D rotation is discussed below.

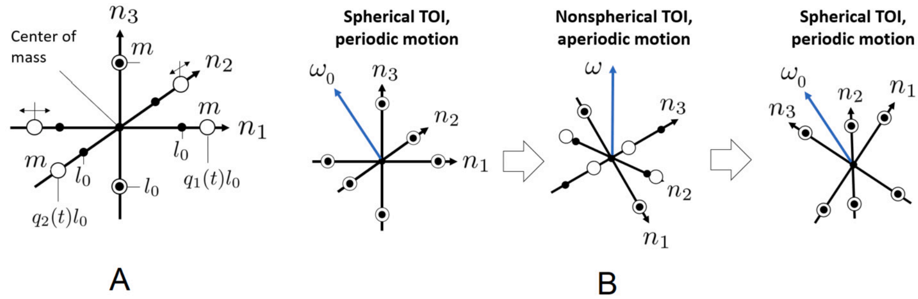

Fig. 1. A) Geometric interpretation of control parameters $q_1(t), q_2(t)$. For the system on the image, $I_0 = 4ml_0^2$. (B) The schematics of an arbitrary angular maneuver.

Here $q_1(t)$ and $q_2(t)$ are independent control parameters that can be manipulated within a certain range between $q_{min} < 1$ and $q_{max} > 1$, to achieve the desirable maneuvering; I_0 is the baseline spherical TOI. Note that in case when $q_1(t) = 1$, $q_2(t) = 1$, the TOI is spherical. Fig. 1 (A) offers a simple mechanical interpretation of the coefficients $q_1(t)$ and $q_2(t)$, highlighting one possible way of technical implementation (alternative ways are discussed in Section 4).

It is easy to see that certain changes in the TOI of a rotating body can be achieved with zero work of centrifugal forces. For example, the body rotating precisely around its principal axis can be arbitrarily transformed (stretched, split, etc.) along this principal axis, as long as the mass distributions around the other two axes remain the same. The other changes may be associated with positive/negative work done to move masses in the field of centrifugal forces.

Simple physical considerations lead us to the conclusion that $q_1(t)$ and $q_2(t)$ should be twice differentiable functions with bounded second derivatives, which ensures that the transformation of the TOI can be done using finite forces/power. For illustration, consider the case when the device depicted in Fig. 1 (A) rotates around n_3 with the angular velocity ω_0. Then the total force F_i, acting on the mass moving along n_i ($i = 1, 2$) toward the center of mass, and instantaneous power developed by this force W_i are given by:

$$F_i = ml_0 \left(\frac{d^2 q_i}{dt^2} + \omega_0^2 q_i \right), \qquad W_i = ml_0^2 \frac{dq_i}{dt} \left(\frac{d^2 q_i}{dt^2} + \omega_0^2 q_i \right) \tag{6}$$

These functions can be seen as the upper bounds defining the necessary capacity of the electromechanical system altering the TOI.

Below we choose the profiles $q_1(t)$, $q_2(t)$ to be the cubic splines connecting equispaced reference values (see Section 3).

The usual convention in rigid body mechanics is the numbering of TOI's principal components I_1, I_2, I_3 in the order of their decrease. In the case of changing principal components, this convention is not useful. In this work indices 1, 2, 3 do not imply order, rather, the minor, major, and intermediate axes are explicitly identified if necessary. Also, in the case when at least one of the control parameters q_i is equal to 1, the principal directions are not uniquely defined. For example, if $q_1(t) = 1$, $q_2(t) = 1$, any axis of rotation is the body's principal axis. In our text we'll use the term "principal axis" only for the directions that remain principal directions of the body for any values of $q_1(t)$, $q_2(t)$.

As mentioned above, the choice of limits for $q_1(t)$ and $q_2(t)$ ensures that the spherical TOI is available. It is therefore possible to stabilize the motion around a fixed axis by making the TOI spherical. This dictates the scheme of the maneuver, depicted in Fig. 1 (B). Here and below we will define the "orientation" (θ, ϕ) as the two angles determining the direction of angular velocity ω in the own spherical coordinate system of the body (defined such that $\mathbf{n}_1$ corresponds to $(\pi/2, 0)$, $\mathbf{n}_2$ – $(\pi/2, \pi/2,)$, $\mathbf{n}_3 = \mathbf{n}_1 \times \mathbf{n}_2$). It is worth noting here that the orientation defined in this way can be interpreted as the angles of "latitude" and "rotation" of a camera, directed along n_3, while the "azimuth" of a camera is given by $\omega_0 t + C$ (see Fig. 6 (A) and the corresponding discussion below). The maneuver starts at a certain state with the spherical TOI I_0, angular velocity ω_0, and the orientation $(\theta_{beg}, \phi_{beg})$. In case the initial angular velocity is not aligned with one of the principal axes, the changes in the TOI initiate complex aperiodic motion. The sequence of changes ends with the state with a spherical TOI I_0 again, characterized by the angular velocity ω_{end}, orientation $(\theta_{end}, \phi_{end})$. The conservation of angular momentum ensures that $\omega_{end} = \omega_0$ (during the maneuver, however, the angular velocity varies). The sequence of TOI changes is found by the optimization procedure that ensures the desired $(\theta_{end}, \phi_{end})$. The optimization technique is described below.

It is important to note that if the body rotates precisely around one of its principal axes, the changes $q_i(t)$ can not perturb the periodic motion. In such a case, the principal axis, aligned with the angular velocity, can be transformed into an intermediate axis, which causes instability (see, e.g. [15]), and rapid development of the misalignment. Therefore, the described system of maneuvering practically does not have the deadlock states.

The rigorous justification of the existence and uniqueness (non-uniqueness) of the sought maneuver trajectory remains beyond the scope of this work. However, our numerical results demonstrate that the optimization algorithm, given proper maneuver parameters search space, always finds the maneuver leading precisely to the desired state, even for transitions between the states with close alignment of the axis of rotation with the principal axes.

Rotational motion of a body that changes its TOI Based on the considerations above, we accept the following assumptions on the rotational motion of the body changing its TOI:

- We consider C^2-continuous evolution of TOI's principal values, given by (5).
- The TOI and its first time derivative are prescribed precisely in the local (rotating) coordinate system at every moment.

The equations of motion are obtained straightforwardly by a generalization of the standard derivation of Euler's equations of rigid body rotation. These equations are obtained from the condition of conservation of angular momentum in the absence of external moments:

$$\dot{\mathbf{L}} = 0 \tag{7}$$

Expansion of the time derivative in (7) leads to the following equation for the rotational motion of a body changing its TOI in the local (rotating) frame, co-oriented with the principal axes of the body:

$$\dot{\mathbf{I}}^l(t)\boldsymbol{\omega}^l(t) + \mathbf{I}^l(t)\dot{\boldsymbol{\omega}}^l(t) + \boldsymbol{\omega}^l(t) \times \mathbf{I}^l(t)\boldsymbol{\omega}^l(t) = 0 \tag{8}$$

Here $\mathbf{I}^l(t)$, $\dot{\mathbf{I}}^l(t)$, $\boldsymbol{\omega}^l(t)$, and $\dot{\boldsymbol{\omega}}^l(t)$ are the TOI, its time derivative, angular velocity and its time derivative in the local frame. The derivation of this equation, its coordinate form in the inertial frame, and the employed algorithm of its numerical solution are discussed in the Supplementary Information.

Dimensionless system of units It is natural to introduce the dimensionless quantities characterizing the maneuver. The following system of units is utilized below. Moments of inertia are measured in $I_0 = 4ml_0^2$, and angular velocities in ω_0. This naturally introduces units of time ($t_0 = 2\pi/\omega_0$), space (l_0) angular momentum ($I_0\omega_0$) and energy ($I_0\omega_0^2/2$). The remaining quantities characterizing the system (N, q_1, q_2) are dimensionless. The time derivatives $\dot{q}_i$, $\ddot{q}_i$ used below are taken with respect to dimensionless time t/t_0. The dimensionless duration of the maneuver $T = (t_{end} - t_{beg})/t_0$, number of reference points N and the span $[q_{min}, q_{max}]$ define the parameter space where the optimal maneuver is sought.

Simulation-guided optimization procedure The procedure to perform an optimization-based search for the control parameters providing the desired maneuver is similar to the one recently suggested by the author and his colleagues in the work [16]. We seek to find the control parameters $q_1(t)$, $q_2(t)$, providing the maneuver highlighted in Fig. 1 (B).

To guide the body toward the desired final orientation (θ, ϕ), we use the following definition of the functional:

$$\begin{gathered}
\mathcal{L}(\theta, \phi, \theta_{goal}, \phi_{goal}) = \arccos(\mathbf{p}(\theta, \phi)\mathbf{p}_{goal}(\theta_{goal}, \phi_{goal})), \\
\mathbf{p}(\theta, \phi) = \begin{pmatrix} \sin\theta\cos\phi \\ \sin\theta\sin\phi \\ \cos\theta \end{pmatrix}, \\
\mathbf{p}_{goal}(\theta_{goal}, \phi_{goal}) = \begin{pmatrix} \sin\theta_{goal}\cos\phi_{goal} \\ \sin\theta_{goal}\sin\phi_{goal} \\ \cos\theta_{goal} \end{pmatrix}.
\end{gathered} \tag{9}$$

i.e., we seek to minimize the angle between the current and the desired orientation. Such functional definition does not penalize for the duration of the maneuver, complexity, or rate of change of the TOI, therefore, these parameters should be prescribed to ensure the feasibility of the maneuver. This definition also does not penalize for the energy one needs to "borrow" to accomplish the maneuver and the number of control reference points used. This functional is strictly zero once the body's final orientation (θ, ϕ) precisely matches the goal orientation $(\theta_{goal}, \phi_{goal})$.

The time evolution of coefficients $q_1(t)$, $q_2(t)$ is given by the cubic splines (implemented in [17]). The initial and final nodal values $q_i(t_{beg})$, $q_i(t_{end})$ are fixed to 1 (spherical TOI), initial and final time derivatives $\dot{q}_i(t_{beg})$, $\dot{q}_i(t_{end})$ are fixed to zero ("clamped" boundary conditions). The remaining $2N$ equispaced nodal values $q = (q_1^1..q_1^N, q_2^1..q_2^N)$ are varied in an unbounded and unconstrained multidimensional optimization procedure. The optimizer seeks for a vector of unknowns $\mathbf{X} : X_i \in \mathcal{R}$, which are mapped to $\mathbf{q} : q_i \in [q_{min}, q_{max}]$ in the following way:

$$\mathbf{q}(\mathbf{X}) = \frac{q_{max} + q_{min}}{2} - \frac{q_{max} - q_{min}}{2}\cos\mathbf{X} \tag{10}$$

The Powell optimization algorithm [18], as implemented in [17] is employed to vary the control parameters evolution. The maneuver duration T, the number of reference values N and the range $[q_{min}, q_{max}]$ are chosen empirically outside of the optimization cycle.

3. Results

As a brief illustration of the suggested approach, let us consider the optimization of TOI control parameters to perform arbitrary angular re-orientations of a spinning body.

The dimensionless system of units described above is used. In all the maneuvers considered below, the control parameters are varied between 0.5 and 1.5, leading to the ranges for principal moments of inertia:

$$I_1 \in (0.625, 1.625),\ I_2 \in (0.625, 1.625),\ I_3 \in (0.25, 2.25). \tag{11}$$

The kinetic energy can therefore vary in the range $E \in (0.222, 2.0)$, while the angular momentum is constant and equal to 1.

Table 1
Reference orientations, given in terms of angles (θ, ϕ) and unit direction vectors $\mathbf{p}$ ($\Delta = 10^{-3}$).

Point	θ	ϕ	$\mathbf{p}$
1	$\pi/2$	$\pi/4$	$2^{-1/2}(1,1,0)$
2	$\pi/4$	$\pi/2$	$2^{-1/2}(0,1,1)$
3	$\pi/4$	0	$2^{-1/2}(1,0,1)$
4	$\arccos(3^{-1/2})$	$\pi/4$	$3^{-1/2}(1,1,1)$
5	Δ	0	$(\sin\Delta, 0, \cos\Delta)$
6	$\pi/2$	0	$(1,0,0)$
7	$\pi/2$	$\pi/2$	$(0,1,0)$
8	π	0	$(0,0,-1)$

Every maneuver is the transition between the orientation $i : (\theta_i, \phi_i)$ and orientation $j : (\theta_j, \phi_j)$. As was discussed above, the initial and final points of the maneuver are characterized by unit spherical TOI, while during the maneuver TOI varies. Initial and final orientations can be visualized as points on a unit sphere - see Fig. 2. Table 1 gives the set of points that were chosen to demonstrate the capabilities of the method.

Table 2 summarizes the list of maneuvers considered in this section. The first column gives the maneuver number. The second column gives the maneuver path in terms of reference orientations specified in Table 1. The third column details whether the maneuver is the result of optimization ("O") or a run with the prescribed control parameters ("P"). The fourth column gives the number of control reference points N (the number of optimization parameters is $2N$). The fifth column gives the dimensionless duration of the maneuver T. The sixth column gives the value of the goal functional after convergence of the optimization procedure. The seventh column lists the number of functional evaluations during the optimization procedure (the number of simulation framework runs). The eighth column gives the wall time of the simulation/series of the simulations performed on a single core of CPU Intel Core i9 (6 GHz). The last column gives the link to the video of the maneuver (if available).

Maneuvers 1-4 illustrate the transitions between orientations that are not aligned with the principal axes of inertia.

Maneuver 5 is the single controlled Garriott-Dzhanibekov flip, performed without parameter optimization - see below.

Maneuvers 6-9 are transitions between the orientations close to the principal axes.

Fig. 3 gives the evolution of control parameters, principal moments of inertia and rotational kinetic energy during the maneuvers 1-4. All of these maneuvers were easily achievable with $T = 16$ (time corresponding to 16 periods of rotation for $q_1 = q_2 = 1$) and just one reference point ($N = 1$). Another important observation is that the kinetic energy of the initial and final state matches precisely (the error does not exceed 10^{-4}), meaning that the total work of the internal forces to accomplish the maneuver is always zero.

Fig. 4 details the evolution of control parameters, principal moments of inertia and rotational kinetic energy for the maneuvers 6-9, whose start and/or end orientations are in close vicinity of the principal axes. For these maneuvers, the algorithm also performed beyond expectations. One can not start the maneuver if the rotation is perfectly aligned with the principal axis - any changes of q_1, q_2 will not induce misalignment. However, for the initial offset from the principal axis $\Delta = 10^{-3}\pi$ rad (point 5 in Table 1), it achieves the goal orientation with reasonably good precision (Table 2). It is worth noting that the slow development of misalignment and convergence to the orientation close to a principal axis lead to longer/more complex maneuvers – we had to increase the number of reference points to 5 and increase the dimensionless duration of the maneuvers five times compared to maneuvers 1-4.

One interesting particular case is the controlled Garriott-Dzhanibekov flip - starting from the rotation around the third principal axis and spherical TOI, we transform the axis of rotation into an intermediate axis, by setting

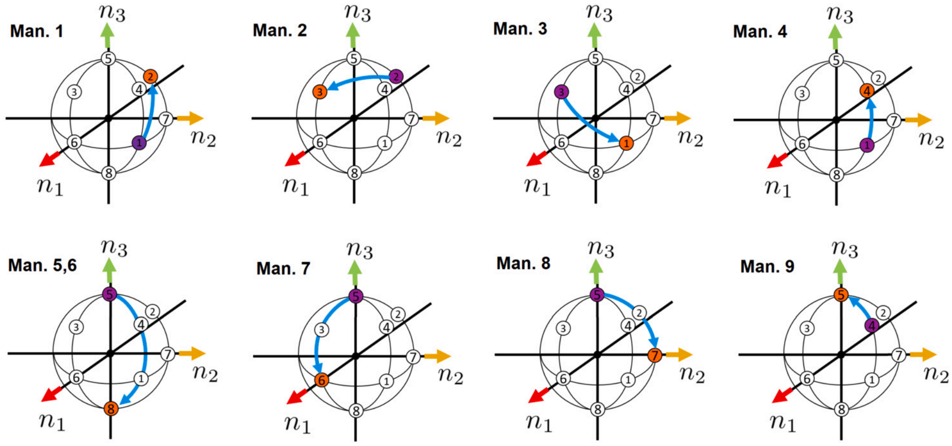

Fig. 2. Schematic representations of paths of re-orientation maneuvers studied. See Table 1 for explicit specification of points coordinates, and Table 2 for the extended description of the maneuvers studied.

Table 2
Benchmark maneuvers and their parameters.

Maneuver	Path	O/P	N	T	$\mathcal{L}(\theta_{end},\phi_{end})$	N_{fev}	T_{comp}	Video
1	1-2	O	1	16	0	434	26:02	[19]
2	2-3	O	1	16	0	322	19:19	[20]
3	3-1	O	1	16	0	392	23:31	[21]
4	1-4	O	1	16	0	771	46:15	[22]
5	5-8	P	-	7.2	3.340×10^{-3}	1	00:02	[23]
6	5-8	O	5	80	5.227×10^{-4}	685	2:51:15	
7	5-6	O	5	80	3.769×10^{-2}	2197	9:09:15	
8	5-7	O	5	80	9.661×10^{-3}	4312	17:58:00	
9	4-5	O	5	80	6.864×10^{-3}	2510	10:27:30	

$$
\begin{aligned}
q_1^2 &= a, \\
q_2^2 &= 2 - q_1^2.
\end{aligned} \tag{12}
$$

Once the first π rad flip is completed, we set $q_1 = 1$, $q_2 = 1$ again and stabilize the rotation. Both changes occur at the moment of alignment of rotation with the third principal axis, and therefore do not cost energy and do not induce misalignment. Our numerical experiment (maneuver 5 in Table 2) demonstrates that the idea of such a maneuver is working [23]. The weak point of such an approach is that in this particular case the changes in the TOI should be instantaneous (or at least sufficiently fast) which, in a light of eq. (7), seems impractical for the applications. The optimization routine addressing the same task (maneuver 6) also resorts to the development of tennis-racket instability, but does it in the relaxed form, with a more complex program of changes of TOI. The optimization problem is, however, ill-posed in this case - the final set of control parameters strongly depends on a small initial misalignment of the rotation axis with the body's principal axis. The same applies for all other maneuvers starting from the angular velocity close to one of the body's principal axes of inertia. Therefore, it seems reasonable to perform such maneuvers in two steps: in the first step, a certain misalignment is produced by the development of tennis racket instability, resulting in the rotation $((\theta_c,\phi_c))$. In the second step, the transition $(\theta_c,\phi_c)\mapsto(\theta_{goal},\phi_{goal})$ is achieved by solving a proper (well-posed) optimization problem. The advantage of such an approach is that the first step should not precisely define intermediate orientation (θ_c,ϕ_c), it is only important to achieve a certain rotation axis, significantly misaligned with the body's principal axes.

Our numerical experiments indicate that achieving the goal orientation co-oriented with one of the principal axes is rather challenging. Fig. 5 (A,B) illustrates the rates of convergence of optimization algorithms for maneuvers 1-4 and maneuvers 6-9. Note that the oscillations of the functional with iteration number is the specific feature of Powell's optimization algorithm, which finds the local minima by bidirectional search in a parameter space along certain directions that are explored sequentially. - see [18] for details. One can see that in the latter case, the convergence to a local minimum is much slower, and the final values are far from zero. Still, these maneuvers converged with reasonably good precision (see Table 2).

Therefore, it is clear that the described approach to angular maneuvering is rather stable and allows to achieve any re-orientation of the spinning body with respect to its angular velocity. Initial alignment of the angular velocity of rotation with the principal axis slows down the maneuver, but can not become a deadlock, since tennis racket instability rapidly develops even from initially tiny misalignment.

Fig. 5 (C) illustrates the quality of angular momentum conservation in our simulations. It can be seen that the quantity that should be precisely constant, in fact, features some drift during numerical motion integration – on the order of 10^{-4} of its absolute value during the longest simulation time period. This can be considered as a sufficiently good quality of time integration, which means the trustworthiness of our simulations.

It is interesting to estimate the dynamic parameters of the described system of angular maneuvering, i.e. the maximum force necessary to move the masses that alter TOI, and the corresponding mechanical power. The dimensionless system of units introduced above leads to the units of force $F_0 = 2ml_0\omega_0^2$ and power $W_0 = \pi^{-1}ml_0^2\omega_0^3$. In these units the expressions (6) take the shape:

$$
\begin{aligned}
F_i &= \frac{1}{2}\left(\frac{\ddot{q}_i}{4\pi^2} + q_i\right), \\
W_i &= \frac{\dot{q}_i}{2}\left(\frac{\ddot{q}_i}{4\pi^2} + q_i\right).
\end{aligned} \tag{13}
$$

Based on the profiles presented in Fig. 3 (A-D), Fig. 4 (A-D), one can evaluate the maximum capacity of the electromechanical system in terms of its maximum achievable force and power. For instance, for the maneuver 1 it results in $F_i^{max} = 1.25$ and $W_i^{max} = 0.045$. For a small CubeSat with $m = 0.2$ kg, $l_0 = 0.1$ m, spinning with the angular veloc-

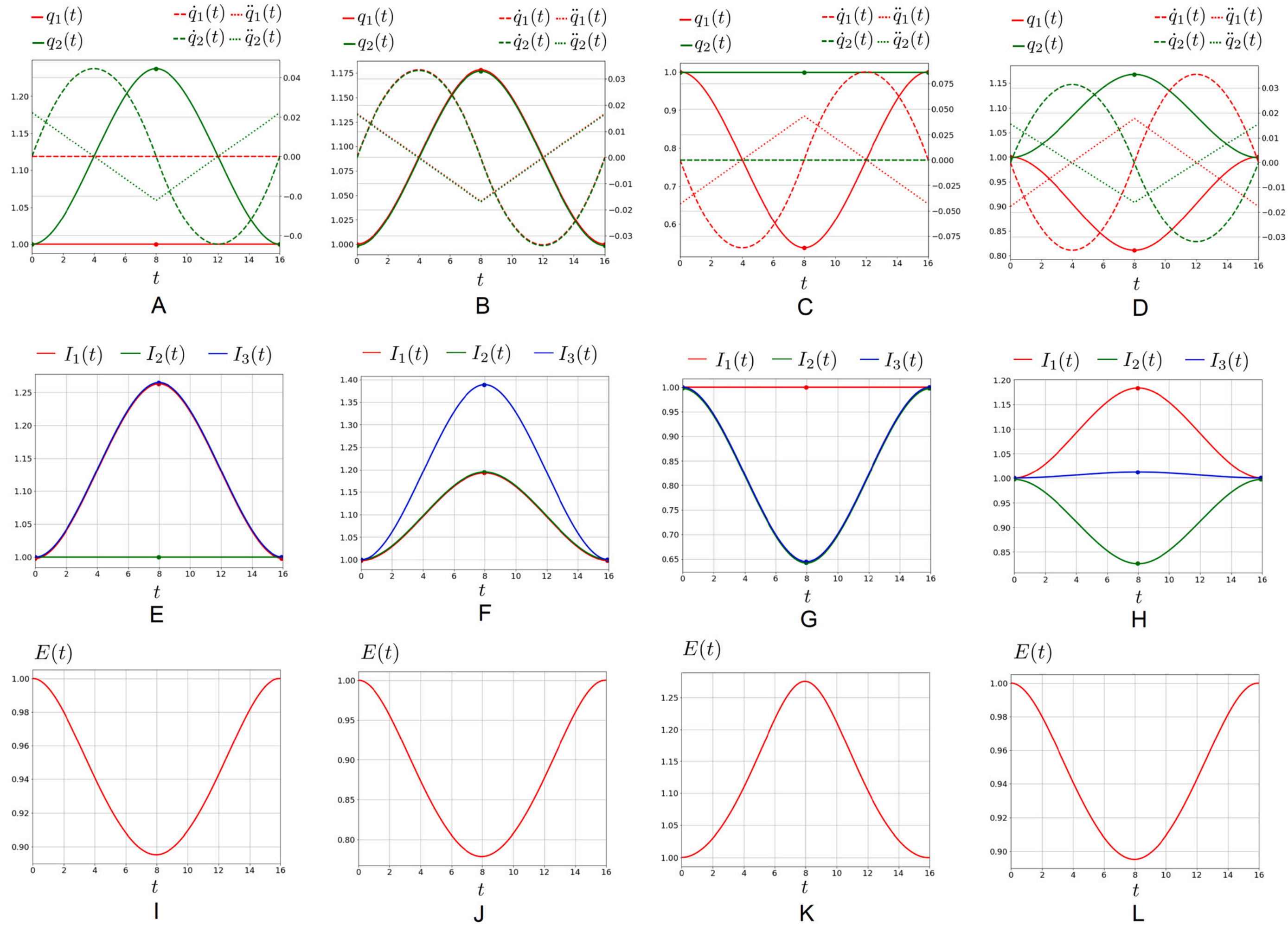

Fig. 3. Time evolution of mass distribution scaling factors q_i and their derivatives $\dot{q}_i, \ddot{q}_i$ (A-D), principal moments of inertia (E-H) and kinetic energies (I-L), corresponding to the (A, E, I) – maneuver 1 [19]; (B, F, J) – maneuver 2 [20]; (C, G, K) – maneuver 3 [21]; (D, H, L) – maneuver 4 [22].

ity $\omega_0 = 10$ Rad/s, these estimates give the force of 2.5 N and power of 143 mWatt, which looks well within the capabilities of modern technology.

It is useful to mention here that all the considered maneuvers (except the maneuver 5) are characterized by negligibly small first term in the force estimate (13), meaning that the centrifugal forces in this case are much larger than the inertial forces associated with translations of masses. This observation tells us that the showcased maneuvers are relatively “soft” and it is technically possible to perform them much faster.

4. Discussion and conclusions

In our work, we approached the idea of attitude control by changing a body’s TOI, which was first highlighted in [7,8] and later developed in [12,1] in the aerospace community. We have suggested a few important advances of this idea, most importantly, the idea of a maneuver that starts and ends at the state of a spherical TOI. This way any arbitrary orientation of a body with respect to its axis of rotation can be stabilized by a certain maneuver, which can be determined by the optimization procedure. This results in essentially new technology of attitude control of a spinning body. It is interesting to note that our orientation parameters (θ, ϕ) admit a simple interpretation. The orientation of a camera or other similar payload (telescope, dipole antenna) directed outward from the center of mass, requires specifying three angular parameters in the static case. However, for a body spinning about the fixed axis, one can alter only two angular parameters, while the third – “azimuth” angle – is prescribed as $\omega_0 t + C$. Simple geometric considerations establish the identity of our orientation angles (θ, ϕ) with the above-mentioned angular parameters, for the case of directed payload aligned with the axis n_3. Fig. 6 (A) illustrates such an interpretation.

The advantage of the approach is that such maneuvers cost practically zero energy (neglecting heat losses in electric circuits and frictional contacts).

These novel ideas can vary in possible technical embodiment. Fig. 6 (B) demonstrates the possible design considered above, that can be compatible with CubeSat design specifications [24]. An extremely important feature of the design is that every mass is not a dead weight but a payload - a massive optical objective of an Earth surveillance camera, chemical batteries and other energy storage devices, etc.

The results above have demonstrated that the controlled development of intermediate axis instability may not be an optimal way to reorient the spacecraft, especially if the duration of the maneuver should be minimized. An alternative approach is to introduce additional axes of possible TOI control, as illustrated in Fig. 6 (C). Such designs are capable of altering TOI beyond our definition of “change” given above, as they allow to instantaneously re-define the directions of principal axes, which enables much faster pre-computed maneuvers to achieve the desirable attitude.

Yet another design illustrated in Fig. 6 (D) showcases two important features of the approach. First, the described change in the TOI can be achieved not only via translation of masses, but their counter-rotations. Second, this design illustrates an idea of a combination of a functional

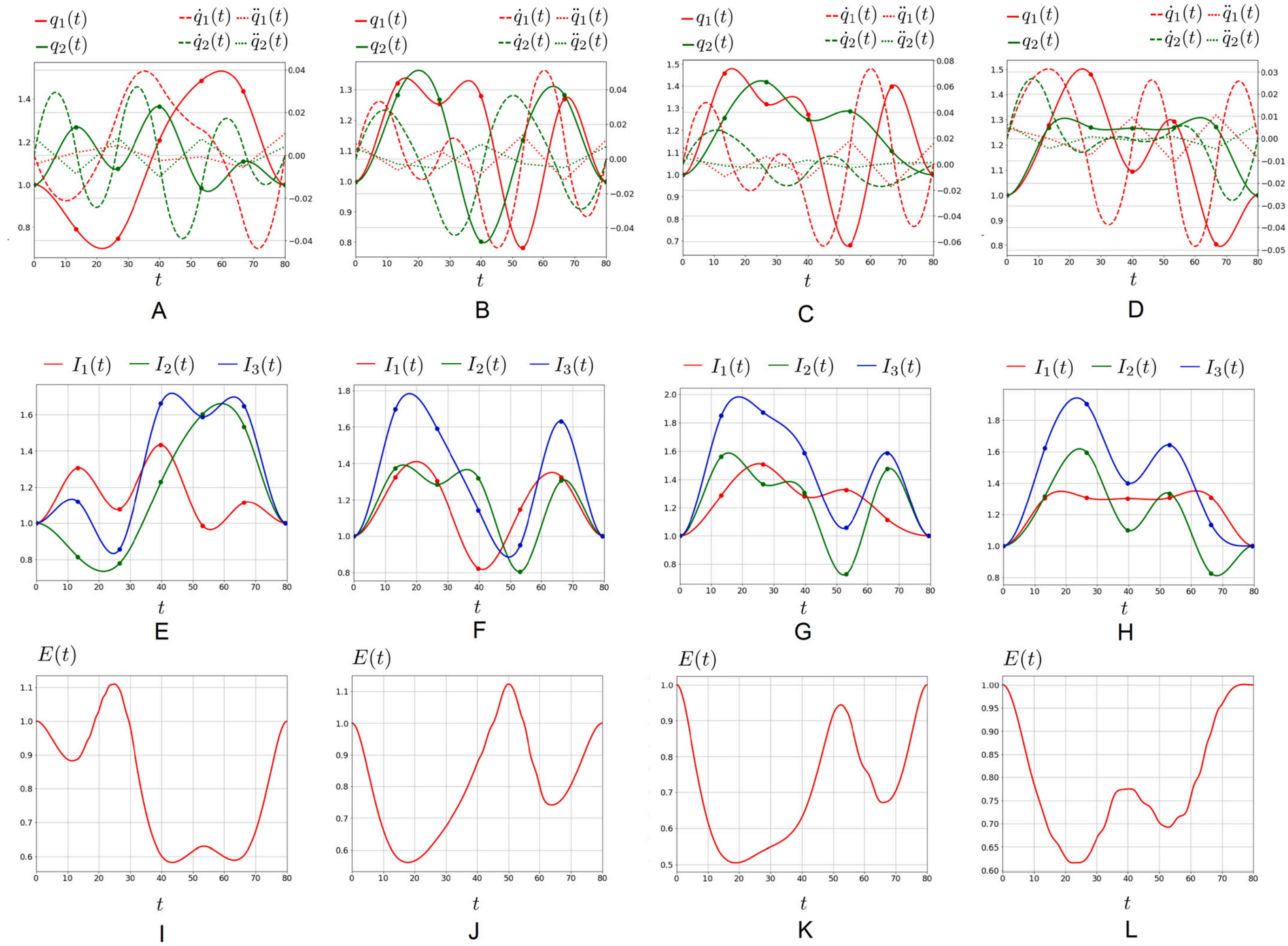

Fig. 4. Time evolution of mass distribution scaling factors q_i and their derivatives $\dot{q}_i, \ddot{q}_i$ (A-D), principal moments of inertia (E-H) and kinetic energies (I-L), corresponding to the (A, E, I) – maneuver 6; (B, F, J) – maneuver 7; (C, G, K) – maneuver 8; (D, H, L) – maneuver 9.

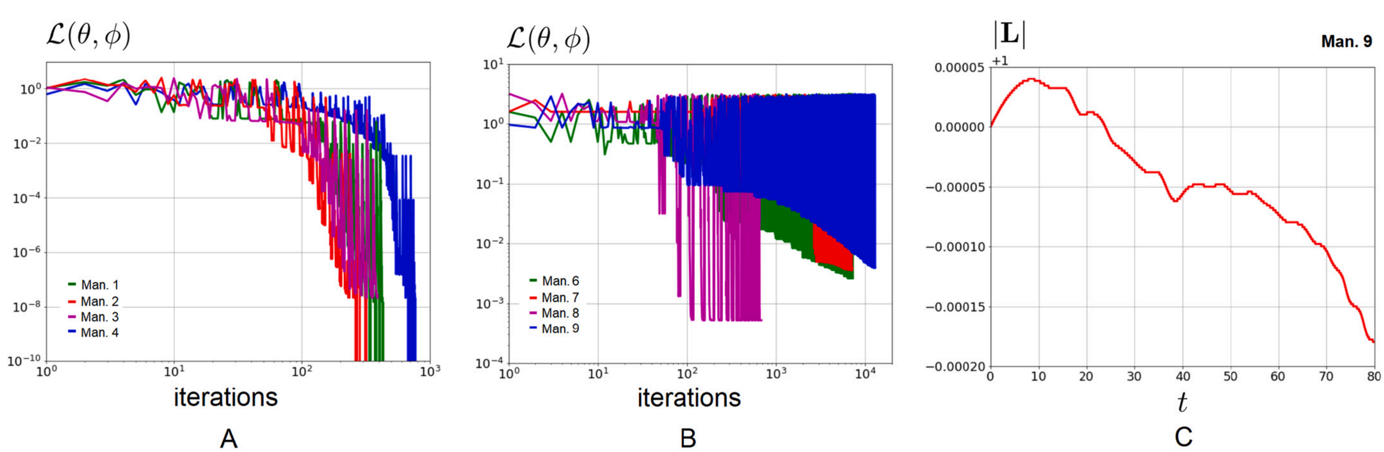

Fig. 5. (A, B) Evolution of the goal functional as the function of the iteration number for (A) maneuvers 1-4, (B) maneuvers 6-9. (C) The drift of angular momentum during the simulation (Maneuver 9).

of a reaction wheel and changing TOI in a single device, depending on whether a co-rotation or counter-rotation of the moving parts is used. Such a design is able to align its axis of rotation of moving parts with the angular velocity by changing TOI, and then stop the rotation of the central shaft by redistributing the angular momentum to the rotating masses acting in a "reaction wheel" mode.

It is easy to see that any number of mass translation or counter-rotation mechanisms does not expand the manifold of available stable orientations, and therefore, any re-orientation available with arbitrarily complex mechanism altering TOI can be achieved by the simplest configuration depicted in Fig. 1 (A) – although, as mentioned above, the more flexible device can perform the required maneuver faster. It is

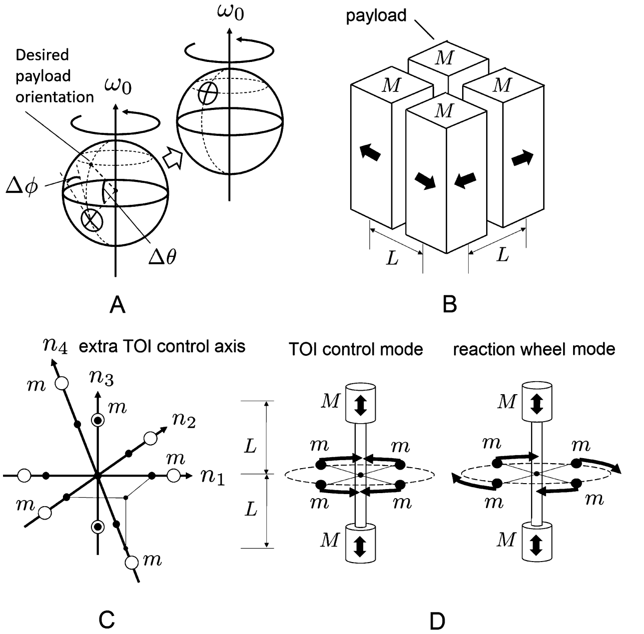

Fig. 6. (A) Positioning a payload by spacecraft re-orientation ($\Delta\theta = \theta_{goal} - \theta$, $\Delta\phi = \phi_{goal} - \phi$). (B) Use the payload to control TOI (similar design is discussed in [1]), (C) Introduce extra axes of TOI control, (D) Design combining functions of TOI control ("Scissors model" according to [1]) and reaction wheel.

also worth noting that stabilizing rotation of a design depicted in Fig. 1 (A) with the prescribed orientation (θ, ϕ) that does not match one of the mass translation axes, is only possible if the TOI is spherical – therefore, our approach is the only one providing arbitrary re-orientation for such a class of designs.

An essential feature of the approach - it can be used in a wide range of angular momenta and self-spin angular velocities - since they only determine the time scale of the maneuver and do not affect its feasibility. Therefore, the same pre-computed maneuver can in principle be performed by a large crewed orbital station and a small, rapidly spinning CubeSat.

Our results suggest that the method can be implemented technologically and used in real spacecraft systems. The numerical simulations indicate that the maneuver can always be found, given the sufficient span of control signals $[q_{min}, q_{max}]$, dimensionless duration T, and complexity (number of reference control points N). The maneuver is resolved with limited precision given insufficient span, duration, and/or complexity, and becomes non-unique if the parameters provided to the optimization procedure are higher than the necessary minimum. Except for the special case of switching between orientations close to the principal axes, the maneuver can be resolved precisely with reasonable T, N, and $[q_{min}, q_{max}]$.

The optimization method showcased in this paper should be viewed only as a proof-of-concept technique, demonstrating that the maneuvering described above is possible. Using modern machine learning/optimization techniques the method can be substantially improved, producing not only precise but shortest and the most energy-efficient maneuvers.

As could be seen above, the calculation of every maneuver requires considerable computational efforts and can not be done on the fly. Therefore, for practical usage one needs to pre-compute and tabulate all meaningful rotations $(\theta_{beg}, \phi_{beg}) \longrightarrow (\theta_{end}, \phi_{end})$. A complete pre-computed table is a five-dimensional array, and its sufficiently dense sampling and storage pose a problem. To address this challenge, one could take a closer look at the structure of the phase space of the rigid motion with the changing TOI, and tabulate this array adaptively. Alternatively, it is possible to use black-box methods, e.g. Tensor Train Cross-approximation [25], in a manner similar to [26], to construct a low-rank representation of the complete table of all possible rotations and the corresponding control signals. Given the symmetric structure of this array and its presumable low-rank structure, the black-box approximation should be a very efficient tool to accelerate necessary pre-computations.

One particularly interesting direction is the exploration of small corrections of the attitude. It can be expected that small adjustments (the functional (9) is initially less than 10^{-1}) could be achieved by fast maneuvers with very few reference points. The larger maneuvers can then be represented as sequences of smaller ones.

In this work, the approach was demonstrated only in the numerical simulation. Further study would certainly require manufacturing the demonstration prototypes designed for gyroscope frames, drop towers, and parabolic flights, which will pave the way to possible experiments with CubeSats and on-board devices like [27], toward practical utilization in larger space systems.

The international patent application (Netherlands patent application 2034951, filed 30.05.23) has been submitted before the publication.

All the codes used in this work are available as part of MercuryDPM software [13,28]. They are located in the developer's branch (https://bitbucket.org/mercurydpm/mercurydpm/src/master) at `/Tools/ChangingTOI/`.

CRediT authorship contribution statement

Igor A. Ostanin: Writing – original draft, Visualization, Validation, Supervision, Software, Project administration, Methodology, Investigation, Formal analysis, Conceptualization. **Matthias Sperl:** Writing – original draft, Validation, Formal analysis.

Declaration of competing interest

The authors declare the following financial interests/personal relationships which may be considered as potential competing interests: Igor Ostanin has patent #N2034951 - METHOD AND SYSTEM FOR CONTROLLING AN ANGULAR ORIENTATION OF A SPINNING BODY pending to University of Twente. If there are other authors, they declare that they have no known competing financial interests or personal relationships that could have appeared to influence the work reported in this paper.

Data availability

The data and codes are freely available via public repository https://bitbucket.org/mercurydpm/mercurydpm/src/master at `/Tools/ChangingTOI/`.

Acknowledgements

The authors thank Prof. Stefan Luding (Multi-Scale Mechanics (MSM), Faculty of Engineering Technology, MESA+, University of Twente) for the fruitful discussions on the topic.

Appendix A. Supplementary material

Supplementary material related to this article can be found online at https://doi.org/10.1016/j.cpc.2024.109181.

References

[1] P.M. Trivailo, H. Kojima, in: L. Dai, R.N. Jazar (Eds.), Inertial Morphing as a Novel Concept in Attitude Control and Design of Variable Agility Acrobatic Autonomous Spacecraft, Springer, Cham, 2022, pp. 119–244.
[2] L. Poinsot, Theorie Nouvelle de la Rotation des Corps, Bachelier, Paris, 1834.
[3] J.R. Wertz, Spacecraft Attitude Determination and Control, 7th edn., Springer, Dordrecht, 1978.
[4] P.C. Hughes, Spacecraft Attitude Dynamics, Dover Publications, New York, 2004.

[5] H.-K. Chen, C.-I. Lee, Anti-control of chaos in rigid body motion, Chaos Solitons Fractals 21 (4) (2004) 957–965, https://doi.org/10.1016/j.chaos.2003.12.034.
[6] L. Van Damme, P. Mardešić, D. Sugny, The tennis racket effect in a three-dimensional rigid body, Phys. D, Nonlinear Phenom. 338 (2017) 17–25, https://doi.org/10.1016/j.physd.2016.07.010.
[7] N.H. Beachley, J.J. Uicker, Reply by authors to L. H. Grasshoff, J. Spacecr. Rockets 6 (10) (1969) 1215–1216, https://doi.org/10.2514/3.59631.
[8] N.H. Beachley, Inversion of spin-stabilized spacecraft by mass translation - some practical aspects, J. Spacecr. Rockets 8 (10) (1971) 1078–1080, https://doi.org/10.2514/3.30349.
[9] T.R. Kane, D. Sobala, A new method for attitude stabilization, AIAA J. 1 (6) (1963) 1365–1367, https://doi.org/10.2514/3.1794.
[10] T.L. Edwards, M.H. Kaplan, Automatic spacecraft detumbling by internal mass motion, AIAA J. 12 (4) (1974) 496–502, https://doi.org/10.2514/3.49275.
[11] V.I. Mayorova, A.S. Popov, S.M. Tenenbaum, O.S. Kotsur, D.A. Rachkin, N.A. Nerovny, N.G. Nazarov, Method for reorientating and controlling the thrust of a rotating spacecraft with a solar sail, Google Patents. WIPO WO2013002673A1, https://patents.google.com/patent/WO2013002673A1/en, 2011.
[12] P.M. Trivailo, Utilisation of the “Dzhanibekov’s effect” for the possible future space missions, in: Proc. of 26-th Int. Symp. Sp. Fl. Dyn., Matsuyama, Japan, 2017, pp. 1–10.
[13] T. Weinhart, L. Orefice, M. Post, M.P. Schrojenstein Lantman, I. Denissen, D.R. Tunuguntla, J.M.F. Tsang, H. Cheng, M.Y. Shaheen, H. Shi, Fast, flexible particle simulations – an introduction to MercuryDPM, Comput. Phys. Commun. 249 (2020) 107129.
[14] P.H. Richter, Regular and chaotic rigid body dynamics, Nonlinear Phenom. Complex Syst. 9 (2) (2006) 115–124.
[15] M.S. Ashbaugh, C.C. Chicone, R.H. Cushman, The twisting tennis racket, J. Dyn. Differ. Equ. 3 (1) (1991) 67–85, https://doi.org/10.1007/BF01049489.
[16] I. Ostanin, H. Cheng, V. Magnanimo, Simulation-guided optimization of granular phononic crystal structure using the discrete element method, Extrem. Mech. Lett. 55 (2022) 101825.
[17] P. Virtanen, S.. Contributors, SciPy 1.0: fundamental algorithms for scientific computing in Python, Nat. Methods 17 (2020) 261–272, https://doi.org/10.1038/s41592-019-0686-2.
[18] M.J.D. Powell, An efficient method for finding the minimum of a function of several variables without calculating derivatives, Comput. J. 7 (1964) 155–162, https://doi.org/10.1093/comjnl/7.2.155.
[19] Supplementary Information, Video of maneuver 1, 2024.
[20] Supplementary Information, Video of maneuver 2, 2024.
[21] Supplementary Information, Video of maneuver 3, 2024.
[22] Supplementary Information, Video of maneuver 4, 2024.
[23] Supplementary Information, Video of maneuver 5, 2024.
[24] CubeSat design specification, https://static1.squarespace.com/static/5418c831e4b0fa4ecac1bacd/t/62193b7fc9e72e0053f00910/1645820809779/CDS+REV14_1+2022-02-09.pdf, 2023.
[25] I.V. Oseledets, Tensor-train decomposition, SIAM J. Sci. Comput. 33 (5) (2011) 2295–2317, https://doi.org/10.1137/090752286.
[26] G. Drozdov, I. Ostanin, I. Oseledets, Time- and memory-efficient representation of complex mesoscale potentials, J. Comput. Phys. 343 (2017) 110–114.
[27] SPHERES mission, https://www.nasa.gov/spheres/home, 2023.
[28] A.R. Thornton, T. Plath, I. Ostanin, H. Götz, J.-W. Bisschop, M. Hassan, R. Roeplal, X. Wang, S. Pourandi, T. Weinhart, Recent advances in mercurydpm, Math. Comput. Sci. 17 (2) (2023) 13, https://doi.org/10.1007/s11786-023-00562-x.

Additional references for Appendix

[29] I. Ostanin, V. Angelidakis, T. Plath, S. Pourandi, A. Thornton, T. Weinhart, Rigid clumps in the mercurydpm particle dynamics code, Comput. Phys. Commun. 296 (2024) 109034, https://doi.org/10.1016/j.cpc.2023.109034.
[30] Itasca Consulting Group Inc., PFC3D (Particle Flow Code in 3 Dimensions). Version 4.0, Itasca Consulting Group Inc., Minneapolis, 2008.